Modelling retinal mosaic development with dendritic outgrowth and lateral cell movement

Stephen J. Eglen

Institute for Adaptive and Neural Computation
Division of Informatics, Univ. of Edinburgh
Scotland EH8 9LW
stephen@anc.ed.ac.uk

Arjen van Ooyen

Netherlands Institute for Brain Research
Meibergdreef 33, 1105 AZ Amsterdam
The Netherlands
A.van.Ooyen@nih.knaw.nl

Abstract

Retinal cells are regularly spaced across the retina and form mosaic-like patterns. The developmental processes involved in producing such mosaics are unclear, although recent evidence suggests that lateral movement of cells may be involved [1]. In this paper, we extend a model of neurite outgrowth [2] to allow cells to move as well as to change their dendritic extent. Starting from random initial positions, cells reorganise into regular mosaics. The network can also dynamically adapt to either increases or decreases in network size during development. Our results support the hypothesis that local cell movement produced by local dendritic interactions can generate regular mosaics.

1 Introduction

A common property of retinal cells is that they are regularly spaced in neural tissue. This regular arrangement ensures that the visual field is processed efficiently and with complete coverage. Many different classes of retinal cells, including cone photoreceptors, horizontal cells and ganglion cells, are all regularly arranged [3]. How do such mosaics arise during development — are newborn cells positioned immediately in a regular fashion across the surface, or do they gradually self-organise from some unordered state? Two lines of recent evidence favours the argument that cells reorganise during development to produce mosaics. First, staining of cholinergic amacrine cells in the rat showed that during migration the cells have no spatial ordering, but then later become regularly spaced within their destination layer [4]. Second, labelling of retinal progenitor cells showed that it is common for certain classes of retinal cells to be tangentially dispersed from their column of origin [1]. Hence it is suggested that lateral cell movement contributes to establishing the regularity of these mosaics.

The forces controlling such tangential cell movement however are still unknown. We suggest that this lateral movement could be the result of repulsive forces between cells. Such repulsive forces were hypothesised as a mechanism for creating mosaics: "identical nerve cells show repulsive action towards each other and an originally random pattern disentangles itself" [3, p457].

1.1 Previous work

Previous theoretical work on retinal mosaics has focused mainly on describing the final mosaic pattern rather than on how the mosaics develop. Two rules have been devised for generating mosaic patterns [5]. In the first, the disturbed triangular lattice rule, cells were initially positioned in a regular hexagonal mosaic and then each cell moved to some random position within a fixed-width radius. By superimposing two independent mosaics generated using this rule, on- and off-centre ganglion cell mosaics could be simulated [6].

In the second rule, the soft disk parking rule, cells were sequentially positioned onto the surface. A tentative position for a new cell was selected at random. The probability of keeping the new cell was a function of distance to its nearest neighbour, following a Boltzmann-like distribution. This rule produced a closer match to horizontal cell mosaics in turtles than the disturbed triangular lattice rule [5]. A simpler ver-

sion of this rule, called the dmin rule [4], rejected new cells if they were closer than some minimum distance (dmin) of its nearest neighbour. The dmin rule replicated both horizontal cell and cholinergic amacrine cell mosaics [7, 4]. The dmin rule has also previously been used in ecological contexts to describe the asynchronous formation of territories amongst animals [8].

As well as these rules, a recent suggestion is that selective ganglion cell death may create mosaics from random cell distributions [9]. Neural activity plays a role in this process, but it is not clear how cells are selected to die.

To our knowledge, the only model proposed for iteratively producing regular distributions from random starting conditions is the synchronous territory model from ecology [8]. At each time step, each unit is moved slightly towards the centre of its Voronoi polygon. (The Voronoi polygon of a unit is the polygon enclosing all points in space that are closer to the unit than to any other unit.) Although this model has never been compared with retinal mosaics, it is likely it will produce good matches to real mosaics. It does not consider the related issue of dendritic field size however.

In this paper, we extend a model previously developed to explore the role of calcium in regulating neurite outgrowth [2]. This model assumed that intracellular calcium levels ($[Ca^{2+}]_i$) controlled cell outgrowth: low levels of $[Ca^{2+}]_i$ promoted outgrowth, whereas high levels promoted retraction of neurites [10]. Cells were initially placed at random in the surface and the resulting neurite size was inversely proportional to the local density of units. We extend this model so that as well as allowing neurites to change size, we also allow cell position to vary according to the relative position of neighbouring cells. In this context, the model applies to only dendrites of retinal cells, rather than their axons.

2 Methods

The model consists of N cells placed within a surface of size 400×400 μm^2. (The size of the surface is arbitrary however since we do not match cell densities and dendritic sizes to values for specific classes of retinal cells.) Each cell is given an initial random position $\mathbf{C}_i$ (bold denotes a 2-d vector) within the surface and a circular dendritic extent of radius $R_i = 0.0\mu$m. The mean membrane potential of cell i, X_i, is given by:

$$\frac{d}{dt}X_i = -\frac{X_i}{\tau} + (1 - X_i)\sum_{j=1}^{N} W_{ij}F(X_j) \qquad (1)$$

$$F(X_j) = \frac{1}{1 + e^{(\theta - X_j)/\alpha}}$$

$$W_{ij} = cA_{ij}$$

where $F(X_j)$ is the mean firing rate of cell j. A_{ij} is the area of overlap between the dendrites of cell i and j. The input from cell j to cell i is A_{ij} multiplied by a constant c, representing synaptic strength. The dendritic extent of each cell, R_i, changes according to its firing rate:

$$\frac{d}{dt}R_i = \rho G(F(X_i)) \qquad (2)$$

$$\text{where} \qquad G(x) = 1 - \frac{2}{1 + e^{(\varepsilon - x)/\beta}}$$

$G(x)$ controls dendrite outgrowth: when the cell's firing rate is below the threshold ε, $G(F(X_i))$ is positive, causing outgrowth. Conversely, when the firing rate is above threshold, $G(F(X_i))$ is negative and the dendrite retracts.

In addition to the above mechanisms used in previous work [2], each cell moves according to the relative positions and size of overlap of neighbouring cells:

$$\frac{d}{dt}\mathbf{C}_i = \eta \sum_{j=1}^{N} u(\mathbf{C}_i - \mathbf{C}_j)W_{ij} \qquad (3)$$

where $u(\mathbf{V})$ is the vector $\mathbf{V}$ normalised to unit length, unless $\mathbf{V} = \mathbf{0}$ (when two cells occupy the same position) in which case $u(\mathbf{V}) = \mathbf{0}$. η controls the rate of movement of each cell. Boundary conditions are imposed such that each unit cannot move beyond the surface (so both elements of $\mathbf{C}_i$ are bounded between [0,400] μm).

The three differential equations for each cell were solved numerically using the Runge-Kutta technique with adaptive step size [11]. Typical simulation parameters were: ($N = 100, \tau = 1.0, \theta = 0.5, \alpha = 0.1, c = 0.6, \varepsilon = 0.6, \beta = 0.1, \rho = 0.001, \eta = 0.1$).

The conformity ratio (CR), a standard measure based upon measuring nearest neighbour distances (NND) amongst cells, was used to evaluate mosaic regularity. The CR is defined as the mean of the NND divided by the standard deviation of the NND [12]. The higher the value, the more regular the mosaic. There is no upper bound for the CR, but typical values for retinal mosaics are 4–9 [3]; values above 3.1 for greater than 50 cells from a square sample are

considered regular at the $P = 0.0001$ confidence level [12]. In contrast, the theoretical mean for random samples is around 1.9.

To exclude sampling errors around the surface edges, NND values are measured only for cells within the central region of the surface[12]. This buffer zone excludes cells at the boundary of our surface which tend to have larger dendrites than the rest of the population. In this paper, cells must have both coordinates in the range [30,370] μm to be in the central region. This typically excludes around a third of our cells from the CR measurements.

3 Results

In this section we present results from the network under normal development and various experimental conditions. Movies of network development are also available on the internet at: http://www.anc.ed.ac.uk/∼stephen/icann99/.

3.1 Normal development

Figure 1(a-d) shows normal development of the network. Starting from random initial positions (1a), cells tend first to extend their dendrites (1b). As dendrites start to overlap, the cells then begin to repel each other, covering the whole space coarsely (1c). Gradually, cells stabilise and form a regular mosaic (1d). The boundary conditions on cell position cause cells at the edge of the surface to have larger receptive fields since they have fewer neighbouring cells than central cells.

Figure 1e shows the increase in mosaic regularity over time. After a thousand seconds, the mosaic is clearly regular as indicated by the high CR value. Although network development time is measured here in seconds, we expect that retinal mosaic development occurs over a longer timescale. Even though cells are free to move anywhere within the surface, they typically tend not to move very far (figure 2).

3.2 Density variations

The density of retinal cells is not constant across the retina, but decreases with eccentricity. To compensate for this decrease in density, the size of receptive fields increases [13]. This is quantified by measuring the (anatomical) coverage factor, defined as the average dendritic area multiplied by the density of cells. Although different classes of retinal cells have different coverage factors (for example, around 1.2 for ganglion cells to around 6 for horizontal cells [13]), the coverage factor for a given class is constant across the retina.

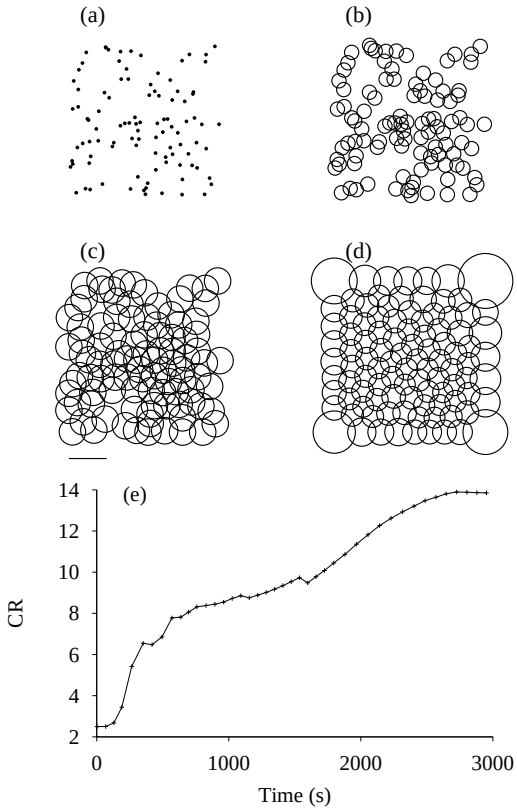

Figure 1: Normal network development. (a-d) Development of dendritic fields and positions. Each circle represents the position of one cell with the radius equal to R_i. Scale bar = 100 μm. (a) Initial conditions. (b) 190 seconds. (c) 350 seconds. (d) 2950 seconds. (e) Increase in mosaic regularity with time.

We therefore tested the network with a wide range of number of cells to see if this affected mosaic development. Figure 3 and table 1 summarise the results. We first find that mosaic regularity is uniformly high (CR $>$ 11) over the wide range of network sizes. However, although the dendritic extent decreases with increasing numbers of cells, the decrease in dendritic field area is not enough to keep the coverage factor constant. (For example, for the data in table 1, when N = 100, the coverage factor is estimated to be 5.3, whereas when N = 400, the coverage factor rises to 9.9.)

These results show that coverage increases with the number of cells in the network, assuming that all other parameters are kept constant.

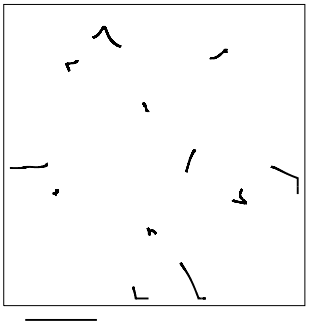

Figure 2: Typical movement of cell position during development. Each trace shows a cell's position during the simulation. This plot shows the traces of 12 typical cells from a network of 100 cells. Scale bar = 100 μm.

However, we find that the coverage factor also varies according to the synaptic strength parameter, c, as shown in table 2 and figure 4. To attain uniform coverage over a wide range of cell densities in our model, the value of c must therefore increase with density.

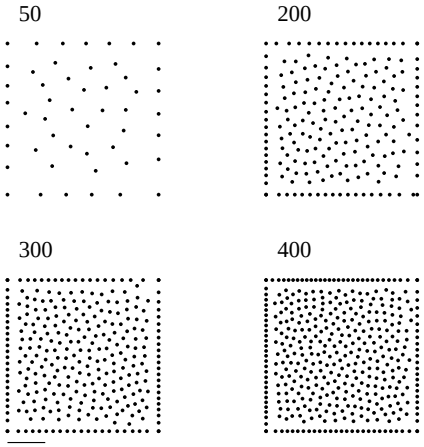

Figure 3: Example final networks using different numbers of cells. Only the cell position is plotted for clarity. (a) N = 50. (b) N = 200. (c) N = 300. (d) N = 400. Scale bar = 100 μm.

3.3 Dynamically changing network size

The retina is robust and can adapt to losing a group of neighbouring cells. After a lesion to a group of retinal ganglion cells in the rat retina, nearby ganglion cells extend their dendrites into the area of the lesion and restore the coverage

N	NND (μm)	R (μm)	CR
50	54.1 $\pm$4.96	63.3 $\pm$1.91	12.0 $\pm$2.6
100	38.1 $\pm$3.40	51.8 $\pm$1.30	11.2 $\pm$0.5
150	31.1 $\pm$2.74	46.6 $\pm$1.19	11.6 $\pm$0.9
200	26.5 $\pm$2.27	43.0 $\pm$0.97	12.0 $\pm$1.2
300	21.7 $\pm$2.12	38.4 $\pm$0.63	13.2 $\pm$0.8
350	20.0 $\pm$1.61	36.8 $\pm$0.71	12.7 $\pm$1.1
400	18.7 $\pm$1.32	35.5 $\pm$0.53	14.2 $\pm$0.8
450	17.6 $\pm$1.28	34.4 $\pm$0.51	13.7 $\pm$0.4

Table 1: Average NND, dendritic extent and CR as a function of cell density. Each value given as mean $\pm$s.d. averaged over five runs from different initial conditions.

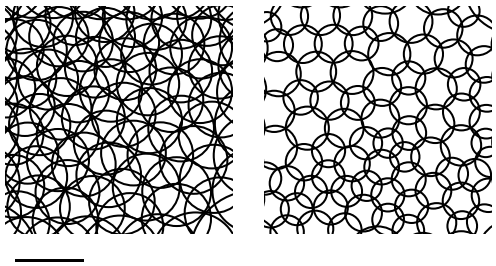

Figure 4: Example dendritic field sizes and overlap when c=1.0 (left) and c=16.0 (right). Only the central portion of each network is shown. Scale bar = 100 μm.

c	R (μm)	Cov	CR
0.1	82.4 $\pm$1.32	13.4 $\pm$0.14	8.9 $\pm$1.2
0.3	61.5 $\pm$1.23	7.44 $\pm$0.10	12.4 $\pm$1.8
0.6	51.7 $\pm$1.38	5.27 $\pm$0.05	13.2 $\pm$2.8
1.0	45.8 $\pm$1.38	4.12 $\pm$0.04	12.3 $\pm$1.3
4.0	33.5 $\pm$1.45	2.21 $\pm$0.03	10.7 $\pm$1.0
8.0	29.4 $\pm$1.81	1.70 $\pm$0.04	10.8 $\pm$2.2
16.0	26.4 $\pm$2.81	1.38 $\pm$0.04	8.7 $\pm$0.8

Table 2: Average dendritic extent, coverage factor (Cov) and CR as a function of synaptic strength (c). Each value given as mean $\pm$s.d. averaged over five runs from different initial conditions (N =100).

of visual space [14]. To test if the model can reproduce this behaviour, a network of 100 cells was developed as normal. Then, after a regular mosaic had formed, a lesion was made by removing ten neighbouring cells from the network (figure 5a). The network then continued to reorganise, and eventually recovered from the lesion (figure 5b): remaining cells immediately neighbouring the lesion invaded the vacant area to cover the surface. Figure 5c shows the mean NND as a function of time. Following the lesion, the mean NND increases slightly to compensate for the loss in cells. Immediately before the lesion, CR=9.5; after recovery from the lesion, CR increased to 10.6.

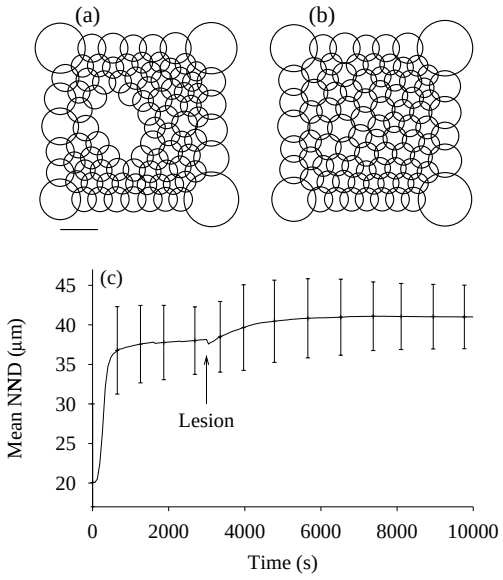

Figure 5: Example lesion experiment (N =100, c=10.0). (a) Network immediately after lesion at 3000s. (b) Reorganised network after recovery from lesion. Scale bar = 100 μm. (c) Plot of mean NND during development, with time of lesion indicated. Error bars indicate ± 1 s.d. of NND.

As well as adapting to losses in cells, the retina handles increases in cell number during the period of cell division and migration. New cells are likely to be added over a period of many days rather than the cells being produced all at once. We therefore tested the network's capacity to reorganise by increasing the number of cells during development. In one experiment, a network with 100 cells was developed for 3000 seconds. Another 100 cells were then added to the network at random positions with R_i = 0. The network adapted to this increase in cell numbers and formed another regular mosaic with smaller NND distances, as shown in figure 6. Just before the increase in network size, CR = 13.1. After recovery from the increase, CR was restored to 12.9. Both lesion and growth experiments were repeatable using different initial conditions and numbers of cells.

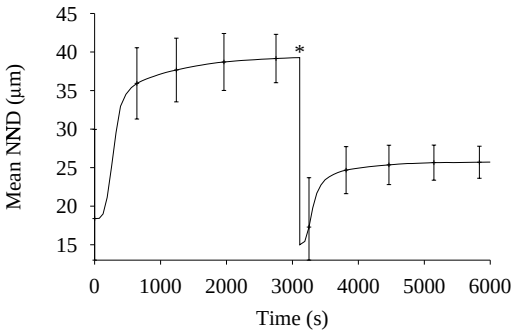

Figure 6: Plot of NND over time for a network that starts with 100 cells and once organised, as marked by asterisk, gains another 100 cells. Error bars indicate ± 1 s.d. of NND.

4 Discussion

Our model demonstrates that local displacements of cells are sufficient to reorganise randomly positioned cells into regular mosaics similar to those found in the retina. The model also adapts to changes in network size during development. We assume that cells move under the influence of dendritic interactions from neighbouring cells. Further work is needed however to see whether such interactions occur in the developing retina — currently the forces causing lateral cell movement are unknown [1].

Our model improves on earlier work by showing how both cell position and dendritic extent develop. However, our model is not complete since it accounts for uniform coverage of the visual space across varying cell densities only if we assume that synaptic strength increases with the density of cells. There are therefore several ways we can extend this work to see if other factors also affect coverage. First, we would like to remove the boundary conditions on cell position by using toroidal surfaces. Second, dendrites of cells could be modelled using a set of processes that extend in different directions around the cell body. This will also allow us to compare the relative importance of cell movement versus elongated dendritic growth in conditions such as recovery from lesions [14].

In this work, we have not tried to specifically model one class of retinal cell mosaic. At present, it is likely that the simulated mosaics are too regular (as indicated by the high CR values) to replicate a specific class of mosaic. Good fits may be attained in future work by adding some random components into the network, for example by adding noise to the direction of cell movement. As well as using the CR measure, other measures such as the distribution of Voronoi polygon areas and the number of nearest neighbours will be used to compare simulated and real mosaics.

Acknowledgements: This work was supported by a Wellcome Trust Mathematical Biology fellowship to S. J. Eglen.

References

[1] B. E. Reese and S-S. Tan. Clonal boundary analysis in the developing retina using X-inactivation transgenic mosaic mice. *Seminars in cell and developmental biology*, 9:285–292, 1998.

[2] A. van Ooyen and J. van Pelt. Activity-dependent outgrowth of neurons and overshoot phenomenon in developing neural networks. *Journal of Theoretical Biology*, 167:27–43, 1994.

[3] H. Wässle and H. J. Riemann. The mosaic of nerve cells in the mammalian retina. *Proceedings of the Royal Society of London Series B*, 200:441–461, 1978.

[4] L. Galli-Resta, G. Resta, S-S. Tan, and B. E. Reese. Mosaics of Islet-1-expressing amacrine cells assembled by short-range cellular interactions. *Journal of Neuroscience*, 17:7831–7838, 1997.

[5] J. Ammermüller, W. Möckel, and P. Rugan. A geometrical description of horizontal cell networks in the turtle retina. *Brain Research*, 616:351–356, 1993.

[6] X. J. Zhan and J. B. Troy. Modeling the mosaics formed by the somata of on- and off-center X retinal ganglion cells. *Investigative Opthalmology and Visual Science*, 37:1057, 1996.

[7] R. Scheibe, J. Schnitzer, J. Rohrenbeck, F. Wohlrab, and A. Reichenbach. Development of A-type (axonless) horizontal cells in the rabbit retina. *Journal of Comparative Neurology*, 354:438–458, 1995.

[8] M. Tanemura and M. Hasegawa. Geometrical models of territory. I. Models for synchronous and asynchronous settlement of territories. *Journal of Theoretical Biology*, 82:477–496, 1980.

[9] G. Jeyarasasingam, C. J. Snider, G. M. Ratto, and L. M. Chalupa. Activity-regulated cell death contributes to the formation of on and off alpha ganglion cell mosaics. *Journal of Comparative Neurology*, 394:335–343, 1998.

[10] S. B. Kater, M. P. Mattson, C. Cohan, and J. Connor. Calcium regulation of the neuronal growth cone. *Trends in Neuroscience*, 11:315–321, 1988.

[11] W. H. Press, S. A. Teukolsky, W. T. Vetterling, and B. P. Flannery. *Numerical Recipies in C*. Cambridge University Press, second edition, 1992.

[12] J. E. Cook. Spatial properties of retinal mosaics: An empirical evaluation of some existing measures. *Visual Neuroscience*, 13:15–30, 1996.

[13] P. Sterling. Microcircuitry of the cat retina. *Annual Review of Neuroscience*, 6:149–185, 1983.

[14] V. H. Perry and R. Linden. Evidence for dendritic competition in the developing retina. *Nature*, 297:683–5, 1982.